Available online at www.sciencedirect.com
SCIENCE DIRECT®
Journal of Process Control 14 (2004) 729–745
JOURNAL OF PROCESS CONTROL
www.elsevier.com/locate/jprocont

Sensitivity analysis for the reduction of complex metabolism models

D. Degenring [a], C. Froemel [b], G. Dikta [c], R. Takors [b,*]

[a] Department of Computer Science, University of Rostock, 18051 Rostock, Germany
[b] Research Center Juelich, Institute of Biotechnology, Forschungszentrum Jülich GmbH, Jülich 52425, Germany
[c] University of Applied Sciences, Aachen/Jülich, Ginsterweg 1, 52428 Jülich, Germany

Abstract

Two different model reduction strategies are studied in order to test their applicability to reduce complex metabolism models. Using a model of one pre-identified model set describing complex metabolic dynamics after glucose pulse stimulation, a model reduction method based on the parameter tuning importance is compared with a pca based approach. Up to 49 of 122 parameters are rejected without significant changes of the simulated trajectories and of the flux distribution.

Applying the reduction procedure to 12 other dynamic models reveals a general model structure inconsistency within the description of the pentose phosphate pathway. That points out the need of additional experiments to reproduce metabolite courses especially of this metabolic pathway.

Thus the sensitivity based model reduction procedure is qualified as a promising tool for the model structure check and can be very useful for the entire model validation process which also includes the critical analysis of the data sets underlying the models.

Keywords: Model reduction; Pca; Parameter sensitivity; Model validation; Metabolism

1. Introduction

The well known, widely-used procaryote *Escherichia coli* K12 possesses approximately 4800 genes encoding 2500 proteins [1]. Several hundreds or even thousands of them are expressed and active at the same time sharing a pool of a comparable number of metabolites, co-factors, nucleotides, etc. Despite this complexity, numerous approaches have been studied up to now to quantitatively describe the cellular metabolism. Stoichiometric models based on flux balance analysis [2], metabolic flux analysis using intensive labelling information [3] or structured metabolism models considering in vitro derived enzyme kinetics [4] are only some of the examples that aim at covering metabolism complexity by modelling.

These approaches have in common that they do not use information about in vivo enzyme kinetics although the knowledge about kinetic and thermodynamic properties of all macromolecules in living cells would offer the possibilities of a *modern* metabolic engineering [5]. In their pioneering work Rizzi et al. [6] aimed at identifying in vivo enzyme kinetic data for *Saccharomyces cerevisiae* by performing glucose pulse experiments. Cells which were cultivated under glucose-limited conditions, were stimulated by a glucose pulse which caused a sudden increase of cellular glucose uptake. As a result, intracellular metabolite pools changed significantly which was monitored during a few minutes time-window by rapid cell sampling combined with immediate metabolism inactivation. Because a series of rapid samples was taken, courses of intracellular metabolite changes were observed which were the basis for the subsequent model identification considering 22 metabolite balances and 99 parameters describing yeast's central metabolism. In the following, similar experiments were performed using *E. coli* [7] and *Zymomonas mobilis* [8].

However, potential pitfalls of the procedure become obvious when the model identifiability and resulting model accuracies are taken into account. The underlying data sets consist of intracellular metabolite concentrations which are only accessible with sophisticated analytical approaches (for instance using LC–MS/MS) considering a significant number of sample preparation steps [9]. As a consequence, dynamically changing metabolite levels of an 'average' cell (neglecting any cell distributions in the population) are given which can

* Corresponding author. Tel.: +49-2461-613365; fax: +49-2461-613870.
E-mail address: r.takors@fz-juelich.de (R. Takors).

0959-1524/$ - see front matter © 2004 Elsevier Ltd. All rights reserved.
doi:10.1016/j.jprocont.2003.12.008

Nomenclature

Metabolites

AcCoA	acetyl-coenzyme A
ADP	adenosindiphosphate
ala	L-alanine
AMP	adenosinmonophosphate
ATP	adenosintriphosphate
BPG	glycerate-1,3-bisphosphate
chor	chorismate
Cit	citrate
DAHP	7-phospho-2-dehydro-3-deoxy-D-arabinoheptonate
DHAP	glycerone phosphate
E4P	D-erythrose-4-phosphate
FBP	β-D-fructose-1,6-bisphosphate
F6P	β-D-fructose-6-phosphate
GAP	glyceraldehyde-3-phosphate
G3P	glycerol-3-phosphate
G6P	α-D-glucose-6-phosphate
ile	isoleucine
kival	α-ketoisovalerate
leu	leucine
mur	subunit of mureine
NAD	diphosphopyridindinucleotide (oxidized)
NADP	diphosphopyridindinucleotide-phosphate (oxidized)
oaa	oxalocetate
PEP	phophoenolpyruvate
2PG	glycerate-2-phosphate
3PG	glycerate-3-phosphate
6PG	6-phospho-D-gluconate
Pyr	pyruvate
R5P	D-ribose-5-phosphate
Ri5P	D-ribulose-5-phosphate
S7P	D-sedoheptulose-7-phosphate
X5P	D-xylulose-5-phosphate

Enzymes

aldo	aldolase
dahps	dahp synthase
eno	enolase
gapdh	glyceraldehyde-3-phosphate dehydrogenase
g3pdh	glycerol-3-phosphate dehydrogenase
g6pdh	glucose-6-phosphate dehydrogenase
pdh	pyruvate dehydrogenase
pfk	phosphofructokinase
pgdh	6-phosphogluconate dehydrogenase
pgi	glucose-6-phosphate isomerase
pgk	phosphoglyceratekinase
pgm	phosphoglyceratemutase
pk	pyruvate kinase
pts	phosphotransferase system
rpe	ribulose-phosphate epimerase
rpi	ribose-phosphate isomerase
ta	transaldolase
tim	triose phosphate isomerase
tka	Transketolase, reaction A
tkb	Transketolase, reaction B

Mathematical terms, variables and subscripts

DE	differential equation
ODE	ordinary differential equation
pca	principal component analysis
t	time
b	metabolite concentration, measured
c	metabolite concentration, simulated
$\mathbf{c}$	vector of all metabolite concentrations, simulated
$\mathbf{c}^0$	vector of all steady-state metabolite concentrations, simulated
$e(\Delta p)$	objective function with respect to a small parameter change
$\mathbf{F}$	parametric Jacobian matrix
g	index, parameter
$\boldsymbol{\Gamma}$	matrix of eigenvectors
γ	eigenvector, represents a column of $\boldsymbol{\Gamma}$
h	index, parameter
i	index, metabolite/variable
j	index, time interval
$\mathbf{J}$	Jacobian matrix
k	index, parameter (and row in $\boldsymbol{\Gamma}$)
λ	eigenvalue
m	total number of independent metabolites/variables
n	total number of time intervals
$\mathbf{N}$	stoichiometry matrix
v	stoichiometric coefficient
$\mathrm{os}(p)$	overall sensitivity with respect to parameter p
p	total number of parameter
$\mathbf{p}$	vector of parameters
Δp	small parameter change
$\mathbf{R}$	covariance matrix
s	normalized, local sensitivity coefficient
$\mathbf{S}$	sensitivity matrix
v	reaction rate
$\mathbf{v}$	vector of rate equations
x	discarded entry of an eigenvector
ζ	error functional

possess significant measurement errors. To build up the structured metabolism model, well-known enzyme databases like (BRENDA [10], ExPASy [11], etc.) are typically used which have the intrinsic problem that their information is usually derived from in vitro enzyme kinetic experiments. The application of these 'in vitro'

approaches for the modelling of in vivo enzyme kinetics turned out to be complicated. Lacking or contradicting enzyme information together with limited experimental possibilities caused the formulation of competing enzyme kinetic equations which need to be identified and qualified within the model identification process. Furthermore, it should be considered that the experimental data sets may not be optimal with respect to the identifiability of all parameters in the complex ODE system [12].

Model reduction thus represents an important step to eliminate redundant parameters and to uncover the most important control mechanisms of the metabolism models. Following this aim, the contribution focusses on the presentation of alternative, classical model reduction approaches which were used to analyze complex metabolism models. Starting basis for the model reduction study are 13 metabolism models. They were selected due to their good fitting quality from in total approximately 200 different models which were formulated recently [13] for the description of the metabolism dynamics in *E. coli* K12 after a glucose pulse [14]. For the sake of clarity, the main reduction results for the selected set of models are summarized briefly whereas the different statistical methods are compared in more detail on the basis of one model. In the following, parameter sensitivity analysis will be based on the criterium of tuning importance as well as on principal component analysis (pca). It will be shown that both approaches lead to comparable results which means that model predictions are still very similar to the original, non-reduced model and the model itself is mechanistically correct. Hence, using the pca approach, the opportunity for an automatic model reduction is given.

2. Modelling

Even if the aim for the evaluation of pulse experiments is to model only certain parts of the whole cellular metabolism, i.e. the glycolysis and the pentose phosphate pathway in this study, it is nevertheless possible to formulate a zoo of varying dynamic models regarding different assumptions concerning the underlying pathway structures or the influences of varying regulatory effectors. Actually 200 different models were fitted to the experimental data. Thirteen models could reproduce most of the experimental trajectories with a reasonable regression quality with respect to the minimal sum of least squares [13]. These models were elected for further model validation, i.e. the model reduction for the model structure check. One of the 13 selected models, namely model 11, is chosen to explain the process of the model development and reduction in the following sections. Another metabolism model, namely model 13, is shown in Appendix A to give an impression, how the model structure and the reduction results vary within the preidentified model set.

2.1. Model structure

The dynamic model includes a system of ordinary differential equations (ODE), which are composed of the mass balance equations for the metabolites:

$$\frac{\mathrm{d}c^i}{\mathrm{d}t} = \sum_{j=1}^{m} v_j^i v_j \quad c^i(t_0) = c^{i,0} \tag{1}$$

where t is the time, c^i denotes the concentration of metabolite i, v_j^i means the stoichiometric coefficient of this species in reaction j and v_j^i is the rate of reaction j.

The mass balance equations of model 11 are given in Table 1 together with a rough visualization of the pathway in Fig. 1. Please note that model 11 represents a simplification of Fig. 1 because some metabolites could not be measured with sufficient analytical accuracy.

2.2. Simplifications within the pentose phosphate pathway

Since it is known, that the interconversions between R5P, Ri5P and X5P are fast enzymatic transformations [15,16], a lumped pool of these compounds (C5P) is formulated, that represents the experimentally determined sum of the concentrations. Following the stoichiometric constraints of the pentose phosphate pathway, this pathway is further simplified as follows:

Table 1
Mass balance equations of model 11

$$\frac{\mathrm{G6P}}{\mathrm{d}t} = v_{\mathrm{pts}} - v_{\mathrm{pgi}} - v_{\mathrm{glp}} - v_{\mathrm{g6pdh}}$$

$$\frac{\mathrm{F6P}}{\mathrm{d}t} = v_{\mathrm{pgi}} - v_{\mathrm{pfk}} - v_{\mathrm{mur}} + v_{\mathrm{FBPase}} + 2 \cdot v_{\mathrm{tkata}}$$

$$\frac{\mathrm{FBP}}{\mathrm{d}t} = v_{\mathrm{pfk}} - v_{\mathrm{aldo}} - v_{\mathrm{FBP-BM}} - v_{\mathrm{FBPase}}$$

$$\frac{\mathrm{GAP}}{\mathrm{d}t} = v_{\mathrm{aldo}} - v_{\mathrm{GAP-PEP}} - v_{\mathrm{Ser}} + v_{\mathrm{tim}} + v_{\mathrm{tkata}}$$

$$\frac{\mathrm{DHAP}}{\mathrm{d}t} = v_{\mathrm{aldo}} - v_{\mathrm{g3pdh}} - v_{\mathrm{tim}}$$

$$\frac{\mathrm{G3P}}{\mathrm{d}t} = v_{\mathrm{g3pdh}} - v_{\mathrm{gly}}$$

$$\frac{\mathrm{PEP}}{\mathrm{d}t} = v_{\mathrm{GAP-PEP}} - v_{\mathrm{pk}} - v_{\mathrm{pts}} - v_{\mathrm{dahps}} - v_{\mathrm{PEP-BM}} - 5 \cdot v_{\mathrm{dahps}}$$

$$\frac{\mathrm{Pyr}}{\mathrm{d}t} = v_{\mathrm{pk}} - v_{\mathrm{pdh}} + v_{\mathrm{pts}}$$

$$\frac{\mathrm{6PG}}{\mathrm{d}t} = v_{\mathrm{g6pdh}} - v_{\mathrm{pgdh}} - v_{\mathrm{pghl}}$$

$$\frac{\mathrm{C5P}}{\mathrm{d}t} = v_{\mathrm{pgdh}} - 3 \cdot v_{\mathrm{tkata}} - v_{\mathrm{rppk}} - 4 \cdot v_{\mathrm{dahps}}$$

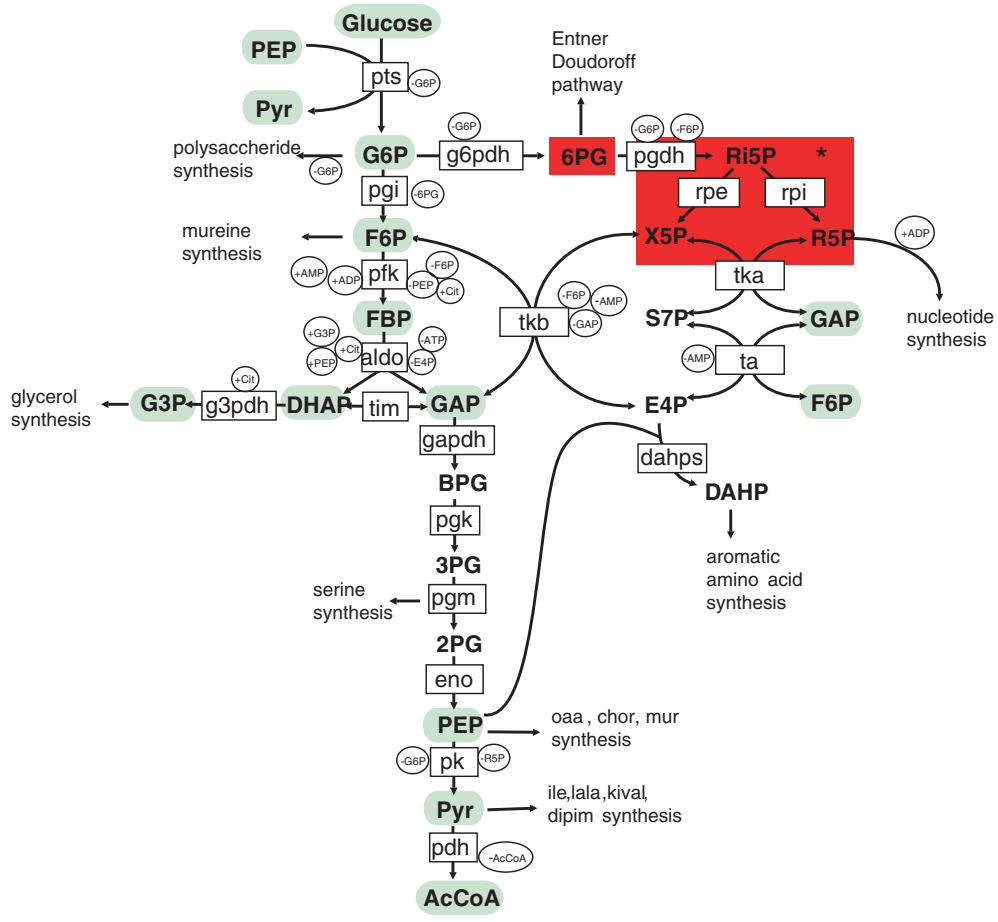

Fig. 1. Reaction network of the glycolysis and pentose phosphate pathway of *Escherichia coli* K12: (squares) enzyme activities; (circles) known regulatory effects; [underlying light gray (blue in web version) boxes] metabolite quantification is possible via enzymatic assay methods [14] and [underlying dark gray (red in web version) boxes] ESI–LC–MS–MS quantification is possible (*via the used HPLC method only the sum of the R5P, Ri5P and X5P concentrations can be determined [9]).

$$\begin{aligned} 2\mathrm{C5P} &\rightleftharpoons \mathrm{GAP} + \mathrm{S7P} \\ \mathrm{GAP} + \mathrm{S7P} &\rightleftharpoons \mathrm{E4P} + \mathrm{F6P} \\ \mathrm{C5P} + \mathrm{E4P} &\rightleftharpoons \mathrm{F6P} + \mathrm{GAP} \\ \hline 3\mathrm{C5P} &\rightleftharpoons 2\mathrm{F6P} + \mathrm{GAP} \end{aligned}$$

The formulation of a differential equation (DE) for the non-measurable component E4P is circumvented by re-defining the reaction into the aromatic amino acid synthesis

$4\mathrm{C5P} + 5\mathrm{PEP} \rightleftharpoons 5\mathrm{DAHP}$ instead of

$\mathrm{C5P} + \mathrm{E4P} \rightleftharpoons \mathrm{DAHP}$

since one C5P molecule is equivalent to 4/5 E4P molecules regarding the number of carbon atoms.

2.3. Simplifications within the glycolysis

The linear reaction sequence, $\mathrm{GAP} \rightleftharpoons \mathrm{BPG} \rightleftharpoons \mathrm{3PG} \rightleftharpoons \mathrm{2PG} \rightleftharpoons \mathrm{PEP}$, is substituted by one combined reaction, $\mathrm{GAP} \rightarrow \mathrm{PEP}$, because the conversions are known to be fast and not significantly affected by regulatory effectors [17–19].

2.4. Rate equations

Often, kinetic rate equations are too complex to be fully identifiable using the data set of the substrate pulse experiment. Hence simplified kinetic equations are used instead. One frequently used example is the multiplicative Michaelis–Menten equation:

$$\frac{\mathrm{d}c^{(3)}}{\mathrm{d}t} = \frac{V_{\max} \cdot c^{(1)} \cdot c^{(2)}}{(K_{m,c^{(1)}} + c^{(1)}) \cdot (K_{m,c^{(2)}} + c^{(2)})} \tag{2}$$

where $c^{(1)}$, $c^{(2)}$, $c^{(3)}$ are the chemical reactants, $V_{\max}$ is the maximal reaction rate and $K_{m,c^{(i)}}$ is the half saturation constant for the respective substrate. This approach is, for instance, well suited to replace complex terms like the irreversibly ordered or ping-pong bi-bi kinetic [20]. Effects of known effectors can be considered by multiplicative terms which are added to the basic form of the

Table 2
Kinetic rate equations of model 11

Phosphotransferase system (v_{pts})

$$k_{f,\mathrm{pts}}\mathrm{Gluc}^{n_{\mathrm{pts},1}}\,\mathrm{PEP}^{n_{\mathrm{pts},2}} - k_{b,\mathrm{pts}}\mathrm{G6P}^{n_{\mathrm{pts},3}}\,\mathbf{Pyr}^{\mathbf{n_{pts},4}}$$

Phosphoglucosisomerase (v_{pgi})

$$k_{f,\mathrm{pgi}}\mathrm{G6P}^{n_{\mathrm{pgi},1}} - k_{b,\mathrm{pgi}}\mathrm{F6P}^{n_{\mathrm{pgi},2}}$$

Polysaccheride synthesis (v_{glp})

$$\frac{V_{f,\mathrm{glp}}\mathrm{G6P}\ \mathrm{ATP}}{(K_{m,\mathrm{G6P,glp}}+\mathrm{G6P})(K_{m,\mathrm{ATP,glp}}+\mathrm{ATP})(\mathrm{G6P}+K_{i,\mathrm{G6P,glp}})^{n_{\mathrm{glp},1}}}$$

Phosphofructokinase (v_{pfk})

$$\frac{2b\cdot D\cdot e\cdot \mathrm{F6P}(\mathbf{1}+\mathbf{FBP})^{\mathbf{2}}\left(\mathbf{1}+\frac{\mathbf{F6P}}{\mathbf{e+1}}\right)}{(\mathbf{e}+\mathbf{1})\left(\mathbf{L}(\mathbf{1}+\mathbf{F6Pc})^{\mathbf{2}}+(\mathbf{1}+\mathbf{FBP})^{\mathbf{2}}\left(\mathbf{1}+\frac{\mathbf{F6P}}{\mathbf{e+1}}\right)^{\mathbf{2}}\right)}\cdot\frac{\mathrm{ATP}}{K_{m,\mathrm{ATP,pfk}}+\mathrm{ATP}}\cdot\frac{\mathbf{ADP}^{\mathbf{n_{pfk,1}}}\mathbf{F6P}^{\mathbf{n_{pfk,2}}}}{(\mathbf{ADP}^{\mathbf{n_{pfk,1}}}+\mathbf{K}_{\mathbf{i,ADP,pfk}}^{\mathbf{n_{pfk,1}}})(\mathbf{F6P}^{\mathbf{n_{pfk,2}}}+\mathbf{K}_{\mathbf{i,F6P,pfk}}^{\mathbf{n_{pfk,2}}})(K_{i,\mathrm{PEP,pfk}}^{n_{\mathrm{pfk},3}}+\mathrm{PEP}^{n_{\mathrm{pfk},3}})}$$

Mureine synthesis (v_{mur})

$$\frac{\mathbf{V_{f,mur}F6P\cdot ATP}}{(\mathbf{K_{m,F6P,mur}}+\mathbf{F6P})(K_{\mathbf{m,ATP,mur}}+\mathbf{ATP})}$$

Fructose 1,6-bisphosphatase (v_{FBPase})

$$\frac{\mathbf{V_{f,FBPase}FBP^{n_{FBPase}}}}{K_{\mathbf{m,FBPase}}^{\mathbf{n_{FBPase}}}+\mathbf{FBP^{n_{FBPase}}}}$$

Aldolase (v_{aldo})

$$\frac{V_{\max,\mathrm{aldo}}\mathrm{FBP}^{n_{\mathrm{aldo},1}}\left(\frac{\mathrm{G3P}}{K_{\mathrm{G3P,aldo}}}\right)^{n_{\mathrm{aldo},2}}}{K_{m,\mathrm{aldo}}^{n_{\mathrm{aldo},1}}+\mathrm{FBP}^{n_{\mathrm{aldo},1}}}$$

Flux of FBP into biomass ($v_{\mathrm{FBP-BM}}$)

$$\frac{\mathbf{V}_{f,\mathbf{FBP-BM}}\mathbf{FBP}^{\mathbf{n_{FBP-BM}}}}{\mathbf{K}_{\mathbf{m,FBP-BM}}^{\mathbf{n_{FBP-BM}}}+\mathbf{FBP}^{\mathbf{n_{FBP-BM}}}}$$

Triosephosphate isomerase (v_{tim})

$$\frac{\left(\frac{V_{f,\mathrm{tim}}\mathrm{DHAP}}{K_{m,\mathrm{DHAP,tim}}}\right)-\left(\frac{V_{b,\mathrm{tim}}\mathrm{GAP}}{K_{m,\mathrm{GAP,tim}}}\right)}{1+\frac{\mathrm{DHAP}}{K_{m,\mathrm{DHAP,tim}}}+\frac{\mathrm{GAP}}{K_{m,\mathrm{GAP,tim}}}}$$

Glycerol 3-phosphate dehydrogenase (v_{g3pdh})

$$\frac{V_{f,\mathrm{g3pdh}}\mathrm{DHAP}_{\mathbf{g3pdh},1}^{\mathbf{n}}\left(\frac{\mathrm{citrate}}{K_{a,\mathrm{Cit,g3pdh}}}\right)^{n_{\mathrm{g3pdh},2}}}{K_{m,\mathrm{DHAP,g3pdh}}^{\mathbf{n_{g3pdh},1}}+DHAP^{\mathbf{n_{g3pdh},1}}}$$

glycerol synthesis (v_{gly})

$$\frac{V_{f,\mathrm{gly}}\mathrm{G3P}^{n_{\mathrm{gly},1}}\left(\frac{\mathrm{F6P}}{K_{a,\mathrm{F6P,gly}}}\right)^{n_{\mathrm{gly},2}}}{K_{m,\mathrm{G3P,gly}}^{n_{\mathrm{gly},1}}+G3P^{n_{\mathrm{gly},1}}}$$

Combined reactions: $v_{\mathrm{GAP-PEP}}=v_{\mathrm{GAPDH}}\cdot v_{\mathrm{PGM}}\cdot v_{\mathrm{PK}}\cdot v_{\mathrm{eno}}$

$$\frac{V_{f,\mathrm{GAP-PEP}}\mathrm{GAP\ NAD\ ADP}}{(K_{m,\mathrm{GAP,GAP-PEP}}+\mathrm{GAP})(K_{m,\mathrm{NAD,GAP-PEP}}+\mathrm{NAD})(K_{m,\mathrm{ADP,GAP-PEP}}+\mathrm{ADP})}$$

Serine synthesis (v_{Ser})

$$\frac{\mathbf{V_{f,Ser}GAP^{n_{Ser}}}}{\mathbf{K}_{m,\mathbf{Ser}}^{\mathbf{n_{Ser}}}+\mathbf{GAP}^{\mathbf{n_{Ser}}}}$$

Pyruvate kinase (v_{pk})

$$\frac{V_{f,\mathrm{pk}}\left(\mathrm{PEP\ ADP}-\frac{\mathrm{Pyr\ ATP}}{K_{\mathrm{eq,pk}}}\right)\left(\frac{K_{i,\mathrm{G6P,pk}}}{\mathrm{G6P}}\right)^{n_{\mathrm{pk},1}}\left(\frac{\mathbf{K_{i,C5P,pk}}}{\mathbf{C5P}}\right)^{\mathbf{n_{pk,2}}}}{A+B}$$

$$A=\mathrm{PEPADP}\left(1+\frac{\mathrm{Pyr}}{K_{i,\mathrm{Pyr,pk}}}\right)+K_{m,\mathrm{ADP,pk}}(\mathrm{PEP}+K_{i,\mathrm{PEP,pk}})+K_{m,\mathrm{PEP,pk}}\mathrm{ADP}$$

(*continued on next page*)

Table 2 (*continued*)

$$B = \frac{V_f}{V_r K_{eq}}\left(K_{m,ATP,pk}\mathrm{Pyr}\left(1+\frac{PEP}{K_{i,PEP,pk}}\right)+\mathrm{ATP}\left[K_{\mathbf{m,Pyr,pk}}\left(\mathbf{1}+\frac{\mathbf{K_{m,PEP,pk}ADP}}{\mathbf{K_{i,PEP,pk}K_{m,ADP,pk}}}\right)+\mathrm{Pyr}\left(1+\frac{ADP}{K_{i,ADP,pk}}\right)\right]\right)$$

Combined reactions from PEP into biomass (v_{PEP-BM})

$$\frac{\mathbf{V_{f,PEP-BM}PEPATP}}{\mathbf{K_{i,PEP,PEP-BM}K_{m,ATP,PEP-BM}}+\mathbf{K_{m,ATP,PEP-BM}PEP}+\mathbf{K_{m,PEP,PEP-BM}ATP}+\mathbf{PEPATP}}$$

Pyruvate dehydrogenase (v_{pdh})

$$\frac{V_{f,pdh}\mathrm{Pyr\ NAD}}{(K_{m,Pyr,pdh}+\mathrm{Pyr})(K_{m,NAD,pdh}+\mathrm{NAD})}\frac{1}{(K_{i,AcCoA,pdh}+\mathrm{AcCoA})^{n_{pdh}}}$$

Glucose-6-phosphate dehydrogenase (v_{g6pdh})

$$\frac{\mathbf{V_{f,g6pdh}G6PNADP}}{(\mathbf{K_{m,NADP,g6pdh}G6P}+\mathbf{K_{m,NADP,g6pdh}K_{i,G6P,g6pdh}})\left(\mathbf{1}+\frac{\mathbf{K_{eq,g6pdh}-NADP}}{\mathbf{K_{i,NADP,g6pdh}}}\right)+\mathbf{NADPG6P}+\mathbf{K_{m,G6P,g6pdh}NADP}}$$

6-Phosphogluconate dehydrogenase (v_{pgdh})

$$\frac{V_{f,pgdh}\left(6PG\ NADP-\frac{C5P}{K_{eq,pgdh}}\right)\left(\frac{K_{i,G6P,pgdh}}{G6P}\right)^{n_{pgdh,1}}}{A+B}$$

$$A = 6PG\ NADP+\mathbf{K_{m,6PG,pgdh}NADP}+\mathbf{K_{m,NADP,pgdh}6PG}$$

$$B = \frac{V_{f,pgdh}}{V_{r,pgdh}K_{eq,pgdh}}\left(K_{m,C5P,pgdh}+C5P\left(1+\frac{6PG}{K_{i,6PG,pgdh}}\right)\right)+\left(\frac{\mathbf{K_{i,F6P,pgdh}}}{\mathbf{F6P}}\right)^{\mathbf{n_{pgdh,2}}}$$

Entner Doudoroff pathway (v_{pghl})

$$\frac{V_{f,pghl}6PG^{n_{pghl,1}}\left(\frac{F6P}{K_{a,F6P,pghl}}\right)^{n_{pghl,2}}}{K_{m,pghl}^{n_{pghl,1}}+6PG^{n_{pghl,1}}}$$

Combined Transketolase and Transaldolase reactions (v_{tkata})

$$\frac{\mathbf{V_{f,tkta}}\left(\mathbf{C5P}-\frac{\mathbf{GAPF6P}}{\mathbf{K_{eq,tkta}}}\right)}{\left(\mathbf{K_{m,C5P,tkta}}+\mathbf{C5P}\left(1+\frac{GAP}{\mathbf{K_{i,GAP,tkta}}}\right)+\frac{\mathbf{V_{f,tkta}}(\mathbf{K_{m,F6P,tkta}GAP}+\mathbf{K_{m,GAP,tkta}F6P}+\mathbf{GAPF6P})}{\mathbf{V_{r,tkta}K_{eq,tkta}}}\right)}$$

Nucleotide biosynthesis (v_{rppk})

$$\frac{\mathbf{V_{f,rppk}C5P^{n_{rppk,1}}}\left(\frac{\mathbf{ADP}}{\mathbf{K_{a,ADP,rppk}}}\right)^{\mathbf{n_{rppk,2}}}}{\mathbf{K_{m,C5P,rppk}^{n_{rppk,1}}}+\mathbf{C5P^{n_{rppk,1}}}}$$

DAHP synthase (v_{dahps})

$$\frac{V_{f,dahps}C5P\ PEP}{(K_{m,C5P,dahps}+C5P)(K_{m,PEP,dahps}+PEP)}$$

Bold written terms are discarded after the sensitivity analysis.

kinetic equations. The resulting equations for the enzyme catalyzed reactions are shown in Table 2.

2.5. Parameter estimation

As most of the published parameter values are obtained from in vitro experiments with purified enzymes and not from experiments performed under physiological conditions, the validity of the values for in vivo cell experiments is questionable. Following information from literature [21] reasonable parameter ranges (between 1 and 10 mM for the saturation constants and 1 and 10 mM s^{-1} for the maximal reaction velocities) are chosen as starting conditions instead of the numerous differing values given for distinct parameters.

The initial conditions for the integration of the dynamic model, i.e. the experimentally determined steady state concentrations, are shown in Table 3. The concentrations of the co-metabolites are not simulated but read in from data material due to the wide range of feasible reactions, in which they participate. This assumption is valid because only the carbon atoms are balanced by the models. The experimentally determined trajectories were approximated by smoothing splines

Table 3
Steady-state concentrations of the metabolites (initial conditions for the integration of the ordinary differential equation system)

Metabolite	Concentration [mM]
G6P	0.16
F6P	0.16
FBP	2.70
GAP	5.57
DHAP	5.01
G3P	0.39
PEP	0.95
Pyr	1.25
6PG	3.66
C5P	1.36

before reading because of the underlying measurement noise. The analytical functions of the weighted cubic B-splines [22] are given in Appendix A together with details about the smoothing algorithm. Simulation and optimization is done using the modelling software MMT [23], whereas the used error functional ζ is defined as follows:

$$\zeta = \frac{1}{n}\sum_{j=1}^{n}\sum_{i=1}^{m}\left(b_j^i - c_j^i\right)^2 \tag{3}$$

where n is the number of the j time intervals, m is the number of the i variables, i.e. metabolites, c_j^i denotes the simulated and b_j^i the experimentally determined metabolite trajectories. As an example, 2318 'measurements' derived from the smoothed data with a time grid of 0.01 s and an observation window from −5 to 18.18 s were used as a data basis to identify model 11 consisting of 122 parameters.

3. Sensitivity analysis

3.1. Local sensitivity functions

Local sensitivities provide the slope of the calculated model output in the parameter space at a given set of values, i.e. here the point of the best parametric estimate.

The effect of a parameter change on the solution in Eq. (1) can be expressed through a Taylor expansion [24]

$$c^i(t, p_g + \Delta p_g, p_{k=1\ldots p,k\neq g}) = c^i(t,\mathbf{p}) + \sum_{k=1}^{p}\frac{\partial c^i(t,\mathbf{p})}{\partial p_g}\Delta p_g + \frac{1}{2}\sum_{l=1}^{p}\sum_{k=1}^{p} \times \frac{\partial^2 c^i(t,\mathbf{p})}{\partial p_h \partial p_g}\Delta p_h \Delta p_g + \cdots \tag{4}$$

A linear approximation of the dependence of the solution on parameter changes is given by the calculation of the first-order partial derivatives $\partial c^i(t,\mathbf{p})/\partial p_g$.

These partial derivatives can be estimated numerically by a finite difference approximation [24,25] changing the gth parameter initially at time t_0 by Δp_g, while the other parameters are held constant. Consequently the sensitivity functions are derived as follows:

$$\frac{\partial c^i(t,\mathbf{p})}{\partial p_g} \approx \frac{c^i(t, p_g + \Delta p_g, p_{k=1\ldots p,k\neq g}) - c^i(t, p_g - \Delta p_g, p_{k=1\ldots p,k\neq g})}{2\Delta p_g} \tag{5}$$

This method of the sensitivity calculation is easy to implement, but the accuracy of the calculated values depends on the parameter change Δp_g. Therefore the sensitivity functions of model 11 are calculated using the direct method to identify an optimal parameter change Δp_g which is small enough to fulfill the assumption of the local linearity of the nonlinear models and which is large enough to avoid numerical round-off errors during simulation.

For this purpose Eq. (1) is formulated in matrix notation as follows:

$$\frac{\mathrm{d}\mathbf{c}}{\mathrm{d}t} = \mathbf{N}\cdot\mathbf{v}(\mathbf{c},\mathbf{p}) \quad \mathbf{c}(0) = \mathbf{c}^0 \tag{6}$$

where t is the time, $\mathbf{v}$ is the vector of the rate equations, $\mathbf{N}$ is the stoichiometric matrix, $\mathbf{p}$ denotes the vector of the kinetic parameters, $\mathbf{c}$ is the vector of the metabolite concentrations and $\mathbf{c}^0$ is the vector of the steady-state concentrations. The parameter variation equation system of ODEs, obtained by differentiating Eq. (6) with respect to the parameter vector, is then integrated simultaneously with Eq. (6)

$$\frac{\mathrm{d}}{\mathrm{d}t}\frac{\partial\mathbf{c}(t,\mathbf{p})}{\partial\mathbf{p}} = D_{\mathbf{p}}\left[\frac{\mathrm{d}}{\mathrm{d}t}\mathbf{c}(t,\mathbf{p})\right] = D_{\mathbf{p}}[\mathbf{N}\cdot\mathbf{v}(\mathbf{c},\mathbf{p})] = \mathbf{N}\cdot\left(\frac{\partial\mathbf{v}}{\partial\mathbf{c}}\frac{\partial\mathbf{c}}{\partial\mathbf{p}} + \frac{\partial\mathbf{v}}{\partial\mathbf{p}}\right) = \mathbf{N}\cdot(\mathbf{J}\cdot\mathbf{S} + \mathbf{F}) \tag{7}$$

where $\mathbf{J}$ is called the Jacobian matrix and $\mathbf{F}$ is called the parametric Jacobian matrix. In contrast to [26], $\frac{\partial\mathbf{c}}{\partial\mathbf{p}}(0) = 0$ is chosen as initial condition for the integration of the ODE system, because the sensitivity functions are employed for the model reduction and not for the calculation of the elasticity coefficients. The sensitivity calculations via the direct method are done using the software MMT2 [27].

Fig. 2 (top graph) shows a comparison of the sensitivity function courses resulting from both calculation approaches with respect to the 'most important' parameter in model 11 (see Section 3.2). In this case the metabolite vector c of Eq. (8) considers the 10 species G6P, F6P, FBP, GAP, DHAP, G3P, PEP, Pyr, 6PG and C5P. As an example, partial derivatives with respect to K_i, *PEP*, *pfk* (see Tables 2 and 4) as p_g of Eq. (8) are shown in Fig. 2. Because of the high similarity of the corresponding courses, it is concluded, that the finite

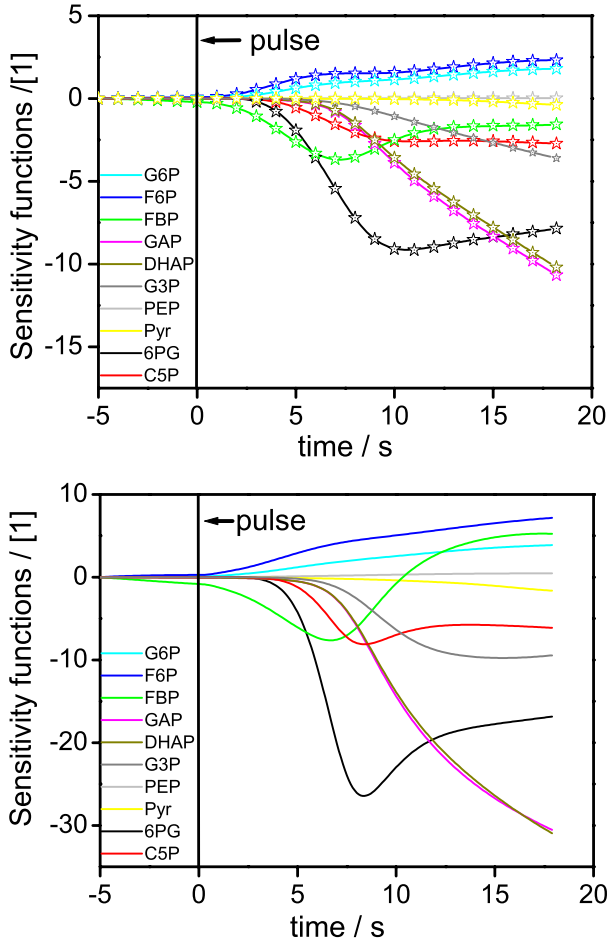

Fig. 2. Sensitivity functions obtained for the variation of parameter $K_{i,\mathrm{pep,pfk}}$ from model 11. (top graph) Sensitivity functions of the original model, continuous lines: sensitivity functions calculated by the finite difference method and stars: sensitivity functions calculated by the direct method and (bottom graph) sensitivity functions of the reduced and re-optimized model calculated by the direct method.

difference approximation using $\Delta p_g = 10^{-5}$ can be chosen to estimate the concentration sensitivities accurately. Therefore this approach was followed in all subsequent studies, since the calculation of the sensitivity functions based on the direct method are very intensive due to the necessary consideration of all cross-dependencies in the complex metabolism model.

In a further calculation step, the sensitivity coefficients are made dimensionless following [28], to allow a comparison of different sensitivity courses:

$$s_k^i(t) = \frac{p_k}{c^i} \cdot \frac{\partial c^i(t,\mathbf{p})}{\partial p_k} = \frac{\partial \ln c^i(t,\mathbf{p})}{\partial \ln p_k} \tag{8}$$

The resulting matrixes, $\mathbf{S}^i$, composed of the normalized local sensitivity coefficients $s_{j,k}^i$ at $j = 1,\ldots,n$ time intervals

$$\mathbf{S}^i = \begin{pmatrix} s_{1,1}^i & \cdots & s_{1,p}^i \\ \vdots & \ddots & \vdots \\ s_{n,1}^i & \cdots & s_{n,p}^i \end{pmatrix} \tag{9}$$

are the basis for the model reduction methods described in the following.

3.2. Tuning importance of the parameters

The study of the normalized sensitivity matrix $\mathbf{S}^i$ allows the identification of a parameter ranking with respect to the effects of initial small parameter changes on the resulting courses of c^i. If several species, c^i, $i = 1,\ldots,m$, are considered, objective functions, $e(\Delta p_g)$, can be introduced [25,29] which represent an integral value of the time-averaged deviations in the trajectories of all species due to small changes of a parameter Δp_g at the initial time t_0. In the present work the sensitivity of the following objective function:

$$e(\Delta p_g) = \sum_{j=1}^{n} \sum_{i=1}^{m} \left[\frac{c_j^i(p_{k=1\ldots p,k\neq g}, p_g + \Delta p_g) - c_j^i(\mathbf{p})}{c_j^i(\mathbf{p})} \right]^2 \tag{10}$$

is calculated by the use of the local concentration coefficients

$$\mathrm{os}(p_g) = \frac{\partial e}{\partial \ln p_g} = \sum_{j=1}^{n} \sum_{i=1}^{m} \left[\frac{\partial \ln c_j^i(\mathbf{p})}{\partial \ln p_g} \right]^2 \tag{11}$$

The sum of squares of the normalized sensitivities is termed overall sensitivity, $\mathrm{os}(p_g)$, and closely connected with the least-square sum, see Eq. (3). The overall sensitivities provide information on the tuning importance of the model parameters, which reflects the effectiveness of parameter changes around their nominal values for the investigated measure, i.e. the objective function.

3.3. Principal component analysis

To decide which parameters can be discarded, we use three methods which are published in [30]. For all three methods the eigenvalues and eigenvectors of $\mathbf{R}^i = \mathbf{S}^{i^{\mathrm{T}}} \cdot \mathbf{S}^i$ are computed. Here, $\mathbf{S}^{i^{\mathrm{T}}}$ denotes the transposed $\mathbf{S}^i$. The eigenvalues, λ_k, are ordered according to their absolute value

$$|\lambda_1| < |\lambda_2| < \cdots < |\lambda_p| \tag{12}$$

and their corresponding eigenvectors are given by

$$\boldsymbol{\Gamma}^i = (\gamma_1, \gamma_2, \ldots, \gamma_p) = \begin{pmatrix} \gamma_{1,1} & \cdots & \gamma_{1,p} \\ \vdots & \ddots & \vdots \\ \gamma_{p,1} & \cdots & \gamma_{p,p} \end{pmatrix} \tag{13}$$

where $\gamma_j = (\gamma_{1,j},\ldots,\gamma_{p,j})^{\mathrm{T}}$, $1 \leqslant j \leqslant p$.

3.3.1. Method 1

Given p^* as the number of parameters to reject, the first p^* eigenvectors, starting with the eigenvector corresponding to the smallest eigenvalue, are considered in turn. The variable, which has the largest component

Table 4
Identified kinetic parameters: originally optimized values and values after the model reduction and re-optimization

Rate equation	Parameter	Value before the reduction	Value after the reduction	unit
v_{pts}	$k_{f,pts}$	4.358	3.269	$mM^{-(n_{pts,1}+n_{pts,2}-1)}\ s^{-1}$
	$n_{pts,1}$	0.996	0.747	1
	$n_{pts,2}$	1.053	1.566	1
	$k_{b,pts}$	0.814	1.218	$mM^{-(n_{pts,3}+n_{pts,4}-1)}\ s^{-1}$
	$n_{pts,3}$	1.183	1.591	1
	$n_{pts,4}$	0.141	–	1
v_{pgi}	$k_{f,pgi}$	0.999	0.994	$mM^{-(n_{pgi,1}-1)}\ s^{-1}$
	$n_{pgi,1}$	0.952	1.405	1
	$k_{b,pgi}$	0.997	0.993	$mM^{-(n_{pgi,2}-1)}\ s^{-1}$
	$n_{pgi,2}$	0.996	1.000	1
v_{glp}	$V_{f,glp}$	1.976	1.886	$mM^{(n_{glp,1}+1)}\ s^{-1}$
	$K_{m,G6P,glp}$	0.991	0.976	mM
	$K_{m,ATP,glp}$	1.133	1.161	mM
	$K_{i,G6P,glp}$	0.626	0.629	mM
	$n_{glp,1}$	0.769	1.262	1
v_{pfk}	b	1.003	1.037	1
	D	0.999	1.065	1
	e	0.999	1.046	1
	L	0.959	–	1
	c	0.998	–	1
	$K_{m,ATP,pfk}$	0.838	0.811	mM
	$n_{pfk,1}$	0.999	–	1
	$K_{i,ADP,pfk}$	0.999	–	mM
	$n_{pfk,2}$	0.981	–	1
	$K_{i,F6P,pfk}$	0.999	–	mM
	$n_{pfk,3}$	14.811	20.104	1
	$K_{i,PEP,pfk}$	0.988	0.984	mM
v_{mur}	$V_{f,mur}$	0.399	–	$mM\ s^{-1}$
	$K_{m,F6P,mur}$	1.786	–	mM
	$K_{m,ATP,mur}$	10.740	–	mM
v_{FBPase}	$V_{f,FBPase}$	0.124	–	$mM\ s^{-1}$
	$K_{m,FBPase}$	68.429	–	mM
	n_{FBPase}	1.960	–	1
v_{aldo}	$V_{max,aldo}$	0.897	0.991	$mM\ s^{-1}$
	$n_{aldo,1}$	3.091	3.203	1
	$K_{m,F6P,aldo}$	4.991	4.601	mM
	$K_{G3P,aldo}$	0.811	0.789	mM
	$n_{aldo,2}$	2.671	2.872	1
v_{FBP-BM}	$V_{f,FBP-BM}$	0.044	–	$mM\ s^{-1}$
	n_{FBP-BM}	5.040	–	1
	$K_{m,FBP-BM}$	8.505	–	mM
v_{tim}	$V_{f,tim}$	1.557	1.513	$mM\ s^{-1}$
	$K_{m,DHAP,tim}$	1.034	1.032	mM
	$V_{b,tim}$	1.114	1.166	$mM\ s^{1}$
	$K_{m,GAP,tim}$	0.834	0.830	mM
v_{g3pdh}	$V_{f,g3pdh}$	1.559	1.783	$mM\ s^{-1}$
	$n_{g3pdh,1}$	1.092	–	1
	$K_{m,DHAP,g3pdh}$	3.812	4.066	mM
	$K_{a,Cit,g3pdh}$	2.072	2.064	mM
	$n_{g3pdh,2}$	5.692	5.900	1
v_{gly}	$V_{f,gly}$	2.947	4.674	$mM\ s^{-1}$
	$n_{gly,1}$	1.592	2.242	1
	$K_{m,G3P,gly}$	1.662	1.609	mM
	$K_{a,F6P,gly}$	1.818	1.782	mM
	$n_{gly,2}$	6.135	5.696	1

(*continued on next page*)

Table 4 (*continued*)

Rate equation	Parameter	Value before the reduction	Value after the reduction	unit
$v_{GAP-PEP}$	$V_{f,GAP-PEP}$	1.929	1.936	$mM\,s^{-1}$
	$K_{m,GAP,GAP-PEP}$	3.672	3.250	mM
	$K_{m,NAD,GAP-PEP}$	4.290	4.069	mM
	$K_{m,ADP,GAP-PEP}$	6.783	6.399	mM
v_{Ser}	$V_{f,Ser}$	0.285	–	$mM\,s^{-1}$
	n_{Ser}	10.551	–	1
	$K_{m,GAP,Ser}$	15.114	–	mM
v_{pk}	$V_{f,pk}$	1.113	1.390	$mM\,s^{-1}$
	$K_{eq,pk}$	0.801	0.778	1
	$K_{i,Pyr,pk}$	1.259	1.884	mM
	$K_{m,ADP,pk}$	1.010	0.760	mM
	$K_{i,PEP,pk}$	0.391	0.341	mM
	$K_{m,PEP,pk}$	1.094	0.826	mM
	$V_{r,pk}$	2.444	3.662	$mM\,s^{-1}$
	$K_{m,ATP,pk}$	0.799	0.609	mM
	$K_{m,Pyr,pk}$	0.107	–	mM
	$K_{i,ADP,pk}$	2.232	3.322	mM
	$K_{i,G6P,pk}$	1.030	1.064	mM
	$n_{pk,1}$	2.074	2.483	1
	$K_{i,C5P,pk}$	1.949	–	mM
	$n_{pk,2}$	0.089	–	1
v_{PEP-BM}	$V_{f,PEP-BM}$	1.321	–	$mM\,s^{-1}$
	$K_{i,PEP,PEP-BM}$	1.246	–	mM
	$K_{m,ATP,PEP-BM}$	41.119	–	mM
	$K_{m,PEP,PEP-BM}$	14.726	–	mM
v_{pdh}	$V_{f,pdh}$	0.996	1.026	$mM^{n_{pdh+1}}\,s^{-1}$
	$K_{m,Pyr,pdh}$	0.996	0.992	mM
	$K_{m,NAD,pdh}$	0.996	0.985	mM
	$K_{i,AcCoA,pdh}$	0.998	0.973	mM
	n_{pdh}	1.696	1.700	1
v_{g6pdh}	$V_{f,g6pdh}$	8.384	–	$mM\,s^{-1}$
	$K_{m,NADP,g6pdh}$	3.533	–	mM
	$K_{i,G6P,g6pdh}$	0.727	–	mM
	$K_{eq,g6pdh}$	2.131	–	mM
	$K_{i,NADP,g6pdh}$	0.145	–	mM
	$K_{m,G6P,g6pdh}$	4.058	–	mM
v_{pgdh}	$V_{f,pgdh}$	0.283	0.222	$mM\,s^{-1}$
	$K_{eq,pgdh}$	1.712	1.811	mM^{-1}
	$K_{m,6PG,pgdh}$	26.696	–	mM
	$K_{m,NADP,pgdh}$	5.813	–	mM
	$V_{b,pgdh}$	1.130	0.883	$mM\,s^{-1}$
	$K_{m,C5P,pgdh}$	3.353	5.018	mM
	$K_{i,6PG,pgdh}$	1.388	1.045	mM
	$K_{i,G6P,pgdh}$	11.543	8.676	mM
	$n_{pgdh,1}$	3.268	2.454	1
	$K_{i,F6P,pgdh}$	24.530	–	mM
	$n_{pgdh,2}$	54.790	–	mM
v_{pghl}	$V_{f,pghl}$	1.551	1.514	$mM\,s^{-1}$
	$n_{pghl,1}$	4.293	7.381	1
	$K_{m,6PG,pghl}$	2.979	3.032	mM
	$K_{a,F6P,pghl}$	1.135	1.143	mM
	$n_{pghl,2}$	7.404	11.977	1
v_{tkata}	$V_{f,tkata}$	1.134	–	$mM\,s^{-1}$
	$K_{eq,tkata}$	1.043	–	mM
	$K_{m,C5P,tkata}$	2.265	–	mM
	$K_{i,GAP,tkata}$	0.810	–	mM
	$V_{r,tkta}$	0.218	–	$mM\,s^{-1}$
	$K_{m,F6P,tkata}$	13.410	–	mM
	$K_{m,GAP,tkata}$	0.868	–	mM

Table 4 (*continued*)

Rate equation	Parameter	Value before the reduction	Value after the reduction	unit
v_{rppk}	$V_{f,\text{rppk}}$	0.308	–	mM s^{-1}
	$n_{\text{rppk},1}$	1.477	–	1
	$K_{m,\text{C5P}}$	2.346	–	mM
	$K_{a,\text{ADP}}$	14.891	–	mM
	$n_{\text{rppk},2}$	2.263	–	1
v_{dahps}	$V_{f,\text{dahps}}$	0.400	0.043	mM s^{-1}
	$K_{\text{C5P,dahps}}$	5.591	16.996	mM
	$K_{\text{PEP,ahps}}$	6.238	17.827	mM

(absolute value) in the considered vector and which has not already been marked, is now selected according to

$$x_1 = \arg\left(\max_{1\leqslant k\leqslant p}|\gamma_{k,1}|\right)$$
$$l>1: x_l = \arg\left(\max_{\substack{1\leqslant k\leqslant p\\ k\neq x_1,\ldots,x_{l-1}}}|\gamma_{k,l}|\right) \tag{14}$$

The p^* columns $\mathbf{x}_l$, $l=1,\ldots,p^*$, of $\mathbf{S}^i$ are marked to reject.

3.3.2. Method 2

Only the eigenvectors corresponding to the p^* smallest eigenvalues are considered. For each of the p parameters the sum of squares of their components in the considered p^* eigenvectors is evaluated and the p^* parameters with the largest amounts are selected

$$x_1 = \arg\left(\max_{1\leqslant k\leqslant p}\sum_{h=1}^{p^*}\gamma_{k,h}^2\right)$$
$$l>1: x_l = \arg\left(\max_{\substack{1\leqslant k\leqslant p\\ k\neq x_1,\ldots,x_{l-1}}}\sum_{h=1}^{p^*}\gamma_{k,h}^2\right) \tag{15}$$

The p^* columns x_l, $l=1,\ldots,p^*$, of $\mathbf{S}^i$ are marked to reject.

3.3.3. Method 3

For this method only $q=p-p^*$ eigenvectors are considered in turn, now starting with the eigenvector corresponding to the largest eigenvalue. The parameter, which has the largest component (absolute value) in the considered vector and which has not already been chosen, is now selected.

$$x_0 = \arg\left(\max_{1\leqslant k\leqslant p}|\gamma_{k,p}|\right)$$
$$l>0: x_l = \arg\left(\max_{\substack{1\leqslant k\leqslant p\\ k\neq x_0,\ldots,x_{l-1}}}|\gamma_{k,p-l}|\right) \tag{16}$$

The q columns x_l, $l=0,\ldots,q-1$, of $\mathbf{S}^i$ are the one to retain.

Hence, methods 1 and 2 focus on the eigenvectors with the lowest eigenvalue, identifying the most important variables and eliminating them. Method 3 follows another strategy by focusing on the most important eigenvector which is then 'liberated' from variables with low input.

The three methods were applied to all m matrices $\mathbf{R}^i$ and only these parameters, which are identified as unimportant in all matrices and by all methods are rejected. The authors want to stress that only this intersection of irrelevant parameters was discarded because parameter importance could be different with respect to the metabolite knot investigated and the pca approach used.

4. Model reduction results

Both, the tuning importance of the parameters described in Section 3.2 and the pca approach described in Section 3.3 were used to reduce model 11 which originally consisted of 122 parameters in 22 reactions. As pointed out above, the strategy was followed to reduce the model such that no significant discrepancies in the prediction of the metabolite courses or resulting reaction rates (fluxes) [31] occurred.

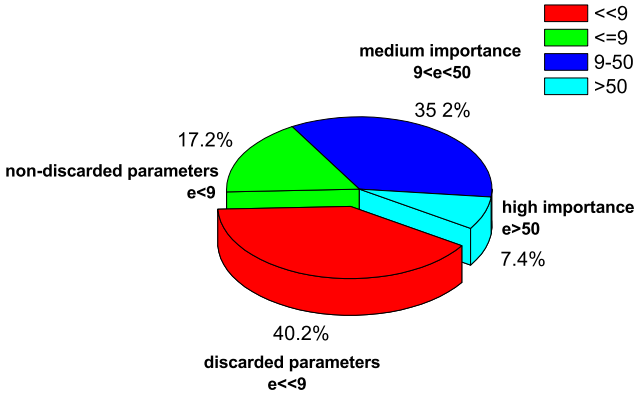

Fig. 3. Distribution of the overall sensitivities os_p of the 122 original parameters in model 11. 49 parameters were discarded because of the low os_p values $\ll 9$. 17.2% (21) parameters possessed low os_p values and were still not rejected. The other parameters showed average and very high tuning performance.

4.1. Model reduction using the parameter tuning importance

As described in Section 3.2 a parameter ranking was identified considering the corresponding overall sensitivity, *os*. Starting at the bottom of the list, parameter values were sequentially set to 0 (or to 1, depending on the respective mathematical expression) and the model simulations were re-started. Parameters, which revealed to possess significant influence on the systems behavior, although their computed overall sensitivity was low, were not discarded and the reduction procedure was continued with the next parameter.

Fig. 3 indicates that, although approximately 35% of all parameters possess a 'medium' importance, only 7.4% of the parameters revealed to be highly important. Here, mainly parameters of the glycolysis and the phosphotransferase system (responsible for the glucose uptake) were found. The inhibition of the phosphofructokinase by PEP turned out to be a dominating effect in glycolysis. Considering $K_{i,\mathrm{PEP,pfk}}$, very high overall sensitivities (up to 600) were calculated, which are one order of magnitude higher than most of the other parameters.

Based on the ranking list 49 parameters with an overall sensitivity up to 8.88 could be eliminated from the model without significant changes on the systems behavior. However, altogether 21 (17.2%) parameters of the pentose phosphate pathway and the pyruvate metabolism which possessed low tuning importance smaller than 9.00, could not be discarded from the model because their influence on model prediction turned out to be too significant. This striking fact was already described elsewhere [32] and was considered to be disadvantageous for the model reduction, because no upper limit for the overall sensitivity values could be given in order to discard all parameters with a smaller value from the model.

4.2. Model reduction using pca

As pointed out above, the model reduction with pca only discarded these parameters which were commonly identified by all three methods. In analogy to the procedure based on parameter's tuning importance, the model prediction after reduction were compared with the original model prediction in order to qualify whether both models are still similar. For this, the error functional ζ of Eq. (3) with respect to the concentrations of the original model, $c^i(t_j, \mathbf{p})$, and the concentrations of the reduced model, $\tilde{c}^i(t_j, \tilde{\mathbf{p}})$, was used.

Fig. 4 indicates that approximately 31 parameters were eliminated without any effect on the model predictions. Then, a set of 12 parameters was discarded at one single reduction step because a complete reaction was identified as non-significant. This caused an increase

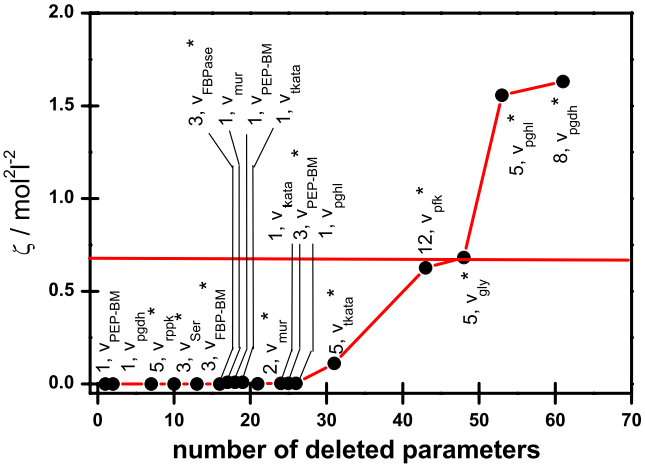

Fig. 4. Error function ζ depending on the number of discarded model parameters in the original model 11. In addition, the number of pca-based discarded parameters and their original reaction rate are indicated by labelling. A star (*) notifies the complete elimination of the reaction rate caused by sequential parameter reduction. The ζ threshold was fixed heuristically such that significant discrepancies of model predictions caused by on-going model reduction, were avoided.

of the ζ value to about 0.6. Subsequent model reduction lead to even more increasing values. Therefore, pca based model reduction was stopped after the elimination of 43 parameters of model 11. Only minor differences between the pca approach and the reduction technique via the overall sensitivities are detected. The reaction catalyzed by the Phosphofructokinase was only partially reduced by the model reduction method following the parameter tuning importance, since an additional constraint, the maintenance of the flux distribution, was considered here besides the error functional ζ. Further on only six parameters coding for a simple model of the oxidative pentose phosphate branch were not yet detected by the pca reduction. Thus we concluded, that the reduction results using the pca approach, as shown in Fig. 4, are basically the same compared with those basing on the overall sensitivities given in Table 2.

4.3. General remarks

The parameters discarded from model 11 are shown in Table 4. It was found that parameter elimination usually coincided with the loss of complete mathematical terms, when original, in vitro kinetic approaches were employed without simplification. From this we concluded that it may be favorable even to start model building with already simplified kinetic expressions. For instance, the models can consider mass action kinetics or alternative terms (see Section 2.4). This holds also true for biomass building reactions, which turned out to be usually a target of model simplification or even complete neglecting (see Table 2).

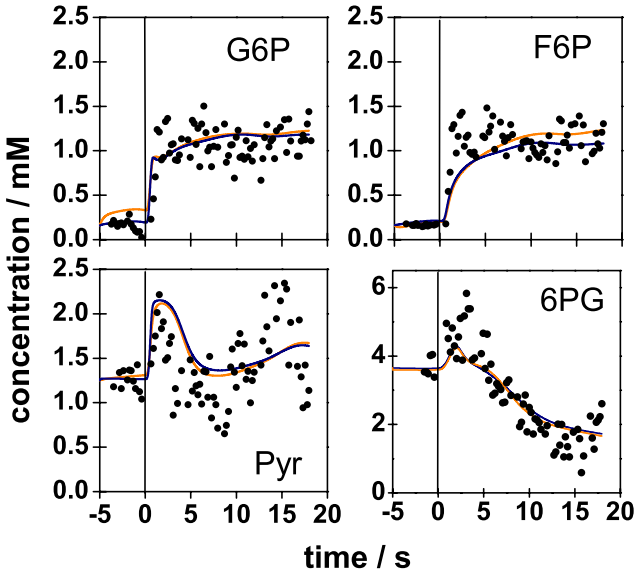

Fig. 5. Time courses of the metabolites: (points) experimental data; [black (blue in web version) lines] simulated trajectories before the model reduction and [gray (orange in web version) lines] simulated trajectories after the reduction.

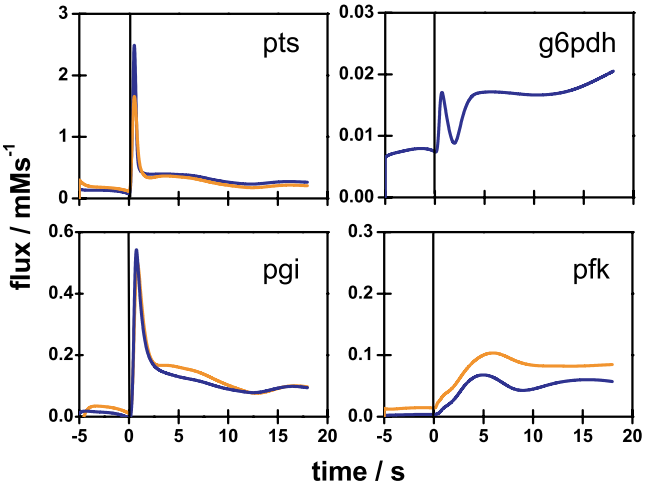

Fig. 6. Time courses of some simulated kinetic rates (fluxes): [black (blue in web version) lines] fluxes simulated before the model reduction; [gray (orange in web version) lines] fluxes simulated after the model reduction; the reaction catalyzed by the glucose-6-phosphate dehydrogenase was eliminated in the reduced model, i.e. the orange line was omitted in the right upper figure).

Although the model structure was strongly simplified by the parameter reduction, the systems behavior did not change significantly. This can be seen for the simulated metabolite trajectories, the courses of G6P, F6P and Pyr are exemplarily shown in Fig. 5, and also for the flux distribution (see Fig. 6). Because the flux into the pentose phosphate had a small value of minor than 0.01 mM s^{-1} before the reduction and all parameters of the g6pdh-catalyzed reaction revealed to be insignificant, the reaction was omitted. For the same reason the combined Transketolase and Transaldolase reactions are eliminated.

In this way the original model is subdivided into one part which describes the pentose phosphate pathway and one describing the glycolysis.

Within the modelling part for the pentose phosphate pathway it turned out that the high steady-state 6PG concentrations of 3.7 mM, as given in Table 3, could be maintained by low exchange fluxes between 6PG and C5P. During the subsequent pulse experiment, the intracellular 6PG and C5P levels even sharply decreased, as shown in Fig. 5. That drop is achieved in the model by the simulation of an enlarged drain off flux into the biomass. Obviously, this part is biologically meaningless. The remaining modelling part for the glycolysis however remains realistic and makes predictions comparable to literature values [33].

To study the general applicability of the model reduction approach, the other twelve models of the preliminary model identification, that was mentioned in Section 2, were reduced as well (see Table 5 for the

Table 5
Results for the model reduction based on the described reduction methods, the models are characterized by the number of differential equations, model parameters and the least square sum, see Eq. (3)

Model		Before the reduction		After the reduction		
No.	Number of DE	Number of parameters	ζ	Number of parameters	ζ before the optimization	ζ after the optimization
1	8	101	1.749	44	2.045	1.523
2	9	105	1.482	35	1.307	1.080
3	9	102	1.189	26	1.264	1.034
4	9	102	1.189	26	1.264	1.026
5	9	102	1.248	26	1.275	0.980
6	9	102	0.951	34	0.944	0.944
7	9	99	1.696	29	1.577	1.302
8	10	122	1.461	73	1.740	1.550
9	10	134	1.087	64	1.508	0.862
10	10	80	1.370	72	1.924	1.372
11	10	122	1.515	73	1.501	1.098
12	9	92	1.151	64	1.151	1.151
13	9	96	0.669	75	1.469	0.814

results). After the reduction the models were re-optimized. Thereby it was observed that the least square sum of the re-optimized, reduced models was smaller than the least square sum of the original parameter fit in many cases. This is ascribed to the better initial situation for parameter fitting especially if a gradient-free, Nelder–Mead Simplex [34] derivative is used, as it is the case for MMT using the subplex method [35].

It was found that all structures could be simplified significantly, for instance leading to the same final structure of the models 3, 4 and 5 in Table 5. Additionally, model reduction revealed that the models 1–8, and 12 all suffer from the same structural problem, namely an interruption of glycolysis by neglecting the Aldolase reaction and Transaldolase/Transketolase reactions after model reduction. Obviously, these models are not meaningful in a biological sense.

Models 9 and 10 have the same model structure problem as model 11, but can also mirror the glycolysis adequately. Summarizing, all these models revealed some difficulties to simulate the metabolite trajectories in the pentose phosphate pathway, which most presumably is caused by the non-physiological, high 6PG level (3.66 mM, which is more than 22-fold higher than the G6P level), that is also in disagreement to values found in literature [33]. This is why it is assumed, that the experimentally determined metabolite courses for 6PG and perhaps also C5P are inconsistent and additional experiments have to be carried out for the reproduction of these trajectories.

Model 13 seems to be most meaningful in a biological sense, because the originally chosen model structure was conserved, see Appendix A. But the low value of the least square sum in Table 5 deceives that only high concentrated metabolites like FBP, DHAP and GAP could be adequately described by the model. The steady-state concentrations and the dynamic courses of the key glycolytic metabolites could not be described equally well.

5. Conclusion

The analysis of the two different model reduction approaches showed that both procedures basically discard the same parameters. However, the pca approach offers the opportunity to be used as a self-controlled routine, meaning that this procedure can be repeated automatically until a predefined upper-limit of the error-functional ζ is achieved. Using the parameter tuning importance, no unique criterium could be identified because even parameters with small parameter tuning importance caused significant model prediction discrepancies. Therefore, this procedure must be performed step-by-step critically studying each model reduction result.

The model reduction procedure based on the two methods enabled to identify severe redundancies and structure problems in the models used. The structure problems in turn indicated the need of additional experiments to reproduce the trajectories of distinct metabolites within the pentose phosphate pathway. This shows the powerfulness of the sensitivity analysis for the validation of mechanistic models in an iterative cycle between data analysis, model building and experimental design.

Acknowledgements

The authors are indebted to Professor C. Wandrey, Research Center Jülich, for supporting this work and the opportunity of using the extensive technical facilities at the Institute of Biotechnology. The authors thank Dr. J. Hurlebaus and M.D. Haunschild, who provided the modelling software MMT and MMT2, respectively, likewise Dr. A. Buchholz for providing the experimental data set. The authors acknowledge financial support from the DFG for project TA241/3-1 and also Professor W. Wiechert and Professor B. Freisleben for the very fruitful cooperation within the DFG project.

Appendix A

A.1. Reduction results for model 13

The modelling and reduction results of model 13 are given in Tables 6 and 7 for the comparison with model 11.

Table 6
Mass balance equations of model 13

$$\frac{\mathrm{G6P}}{\mathrm{d}t} = v_{\mathrm{pts}} - v_{\mathrm{pgi}} - v_{\mathrm{g6pdh}}$$

$$\frac{\mathrm{F6P}}{\mathrm{d}t} = v_{\mathrm{pgi}} - v_{\mathrm{pfk}} + v_{\mathrm{FBPase}} + v_{\mathrm{tkb}} + v_{\mathrm{tkata}}$$

$$\frac{\mathrm{FBP}}{\mathrm{d}t} = v_{\mathrm{pfk}} - v_{\mathrm{aldo}} - v_{\mathrm{FBPase}}$$

$$\frac{\mathrm{GAP}}{\mathrm{d}t} = v_{\mathrm{aldo}} - v_{\mathrm{GAP-PEP}} - v_{\mathrm{Ser}} - v_{\mathrm{tim}} + v_{\mathrm{tkb}}$$

$$\frac{\mathrm{DHAP}}{\mathrm{d}t} = v_{\mathrm{aldo}} + v_{\mathrm{tim}}$$

$$\frac{\mathrm{PEP}}{\mathrm{d}t} = v_{\mathrm{GAP-PEP}} - v_{\mathrm{pk}} - v_{\mathrm{pts}} - v_{\mathrm{dahps}} - v_{\mathrm{PEP-BM}} - v_{\mathrm{dahps}}$$

$$\frac{\mathrm{Pyr}}{\mathrm{d}t} = v_{\mathrm{pk}} - v_{\mathrm{pdh}} + v_{\mathrm{pts}}$$

$$\frac{\mathrm{6PG}}{\mathrm{d}t} = v_{\mathrm{g6pdh}} - v_{\mathrm{pgdh}}$$

$$\frac{\mathrm{C5P}}{\mathrm{d}t} = v_{\mathrm{pgdh}} - v_{\mathrm{tkb}} - 2 \cdot v_{\mathrm{tkata}} - v_{\mathrm{dahps}}$$

$$\frac{\mathrm{E4P}}{\mathrm{d}t} = 2 \cdot v_{\mathrm{tkata}} - v_{\mathrm{tkb}} - v_{\mathrm{dahps}}$$

Table 7
Kinetic rate equations of model 13

Phosphotransferase system (v_{pts})

$$\frac{V_{\max,\mathrm{pts}}\mathrm{Gluc}\ \mathrm{PEP}}{(K_{m,\mathrm{Gluc,pts}}+\mathrm{Gluc})(K_{m,\mathrm{PEP,pts}}+\mathrm{PEP})(K_{i,\mathrm{G6P,pts}}+\mathrm{G6P})^{n_{\mathrm{pts}}}}$$

Phosphoglucosisomerase (v_{pgi})

$$\frac{\left(\frac{V_{f,\mathrm{pgi}}\mathrm{G6P}}{K_{m,\mathrm{G6P,pgi}}}\right)-\left(\frac{V_{b,\mathrm{pgi}}\mathrm{F6P}}{K_{m,\mathrm{F6P,pgi}}}\right)}{1+\frac{\mathrm{G6P}}{K_{m,\mathrm{G6P,pgi}}}+\frac{F6P}{K_{m,\mathrm{F6P,pgi}}}}$$

Phosphofructokinase (v_{pfk})

$$\frac{2D\cdot e\cdot \mathrm{F6P}(1+\mathrm{FBP})^2\left(1+\frac{\mathrm{F6P}}{e+1}\right)}{(e+1)\left(L(1+\mathrm{F6P}c)^2+(1+\mathrm{FBP})^2\left(1+\frac{\mathrm{F6P}}{e+1}\right)^2\right)}\cdot\frac{\mathrm{ATP}}{K_{m,\mathrm{ATP,pfk}}+\mathrm{ATP}}$$

Aldolase (v_{aldo})

$$\frac{V_{f,\mathrm{aldo}}\left(\mathrm{FBP}-\frac{\mathrm{DHAP\ GAP}}{K_{\mathrm{eq,aldo}}}\right)}{K_{m,\mathrm{FBP,aldo}}+\mathrm{FBP}\left(1+\frac{\mathrm{DHAP}}{K_{i,\mathrm{DHAP,aldo}}}\right)+\frac{V_{f,\mathrm{aldo}}}{V_{r,\mathrm{aldo}}K_{\mathrm{eq,aldo}}}(K_{m,\mathrm{GAP,aldo}}\mathrm{DHAP}+K_{m,\mathrm{DHAP,aldo}}\mathrm{GAP}+\mathrm{DHAP\ GAP})}$$
$$\cdot\left(\frac{K_{i,\mathrm{GAP,aldo}}}{\mathrm{GAP}}\right)^{n_{\mathrm{GAP,aldo}}}\left(\frac{K_{i,\mathrm{DHAP,aldo}}}{\mathrm{DHAP}}\right)^{n_{\mathrm{DHAP,aldo}}}\left(\frac{K_{i,\mathrm{E4P,aldo}}}{\mathrm{E4P}}\right)^{n_{\mathrm{E4P,aldo}}}\left(\frac{K_{i,\mathrm{ATP,aldo}}}{\mathrm{ATP}}\right)^{n_{\mathrm{ATP,aldo}}}\cdot\left(\frac{\mathbf{PEP}}{\mathbf{K_{a,PEP,aldo}}}\right)^{\mathbf{n_{PEP,aldo}}}\left(\frac{\mathrm{citrate}}{K_{a,\mathrm{Cit,aldo}}}\right)^{n_{\mathrm{Cit,aldo}}}$$

Triosephosphate isomerase (v_{tim})

$$\frac{\left(\frac{V_{f,\mathrm{tim}}\mathrm{GAP}}{K_{m,\mathrm{GAP,tim}}}\right)-\left(\frac{V_{b,\mathrm{tim}}\mathrm{DHAP}}{K_{m,\mathrm{DHAP,tim}}}\right)}{1+\frac{\mathrm{GAP}}{K_{m,\mathrm{GAP,tim}}}+\frac{\mathrm{DHAP}}{K_{m,\mathrm{DHAP,tim}}}}$$

Combined reactions: $v_{\mathrm{GAP-PEP}}=v_{\mathrm{GAPDH}}\cdot v_{\mathrm{PGM}}\cdot v_{\mathrm{PK}}\cdot v_{\mathrm{eno}}$

$$\frac{V_{\max,\mathrm{GAP-PEP}}\mathrm{GAP}\ \mathrm{NAD}}{K_{m,\mathrm{GAP,GAP-PEP}}K_{m,\mathrm{NAD,GAP-PEP}}+K_{m,\mathrm{NAD,GAP-PEP}}\mathrm{GAP}+K_{m,\mathrm{GAP,GAP-PEP}}\mathrm{NAD}+\mathrm{GAP\ NAD}}$$

Serine synthesis (v_{Ser})

$$\frac{V_{\max,\mathrm{Ser}}\mathbf{GAP^{n_{Ser}}}}{\mathbf{K_{m,Ser}^{n_{Ser}}}+\mathbf{GAP^{n_{Ser}}}}$$

Pyruvate kinase (v_{pk})

$$\frac{\left(\frac{V_{f,\mathrm{pk}}\mathrm{PEP}}{K_{m,\mathrm{PEP,pk}}}\right)-\left(\frac{V_{b,\mathrm{pk}}\mathrm{Pyr\ ATP}}{K_{m,\mathrm{Pyr,pk}}}\right)}{1+\frac{\mathrm{PEP}}{K_{m,\mathrm{PEP,pk}}}+\frac{\mathrm{Pyr\ ATP}}{K_{m,\mathrm{Pyr,pk}}}}$$

Pyruvate dehydrogenase (v_{pdh})

$$\frac{V_{f,\mathrm{pdh}}\left(\mathrm{Pyr\ NAD}-\frac{\mathrm{AcCoA}}{K_{\mathrm{eq,pdh}}}\right)}{\mathrm{Pyr\ NAD}+K_{m,\mathrm{pyr,pdh}}\mathrm{NAD}+K_{m,\mathrm{NAD,pdh}}\mathrm{Pyr}+\frac{V_{f,\mathrm{pdh}}}{V_{b,\mathrm{pdh}}K_{\mathrm{eq,pdh}}}\left(K_{m,\mathrm{AcCoA,pdh}}+\mathrm{AcCoA}\left(1+\frac{\mathrm{Pyr}}{K_{i,\mathrm{Pyr,pdh}}}\right)\right)+\left(\frac{\mathbf{AcCoA}}{\mathbf{K_{i,pdh}}}\right)^{\mathbf{n_{pdh}}}}$$

Fructose 1,6-bisphosphatase (v_{FBPase})

$$\frac{V_{\max,\mathrm{FBPase}}\mathrm{FBP}^{n_{\mathrm{FBPase}}}}{K_{m,\mathrm{FBPase}}^{n_{\mathrm{FBPase}}}+\mathrm{FBP}^{n_{\mathrm{FBPase}}}}$$

Glucose 6-phosphate dehydrogenase (v_{g6pdh})

$$\frac{V_{\max,\mathrm{g6pdh}}\mathrm{G6P\ NADP}}{(K_{m,\mathrm{G6P,g6pdh}}+\mathrm{G6P})(K_{m,\mathrm{NADP,g6p}}+\mathrm{NADP})(K_{i,\mathrm{G6P,g6pdh}}+\mathrm{G6P})^{n_{\mathrm{g6pdh}}}}$$

6-Phosphogluconate dehydrogenase (v_{pgdh})

$$\frac{V_{f,\mathrm{pgdh}}\mathrm{6PG\ NADP}}{K_{ia,\mathrm{pgdh}}K_{m,\mathrm{NADP,pdgh}}+K_{m,\mathrm{NADP,pgdh}}\mathrm{6PG}+K_{m,\mathrm{6PG,pgdh}}\mathrm{NADP}+\mathrm{6PG\ NADP}}$$

Transketolase B (v_{tkb})

$$\frac{V_{f,\mathrm{tkb}}\mathrm{E4P\ C5P}}{(K_{m,\mathrm{E4P,tkb}}+\mathrm{E4P})(K_{m,\mathrm{C5P,tkb}}+\mathrm{C5P})\left(K_{\mathrm{F6P,tkb}}+\frac{\mathrm{F6P}}{K_{i,\mathrm{F6P,tkb}}}\right)^{n_{\mathrm{tkb},1}}}\cdot\frac{1}{\left(K_{\mathrm{GAP,tkb}}+\frac{\mathrm{GAP}}{K_{i,\mathrm{GAP,tkb}}}\right)^{n_{\mathrm{tkb},2}}\left(K_{\mathrm{AMP,tkb}}+\frac{\mathrm{AMP}}{K_{i,\mathrm{AMP,tkb}}}\right)^{n_{\mathrm{tkb},3}}}$$

(*continued on next page*)

Table 7 (*continued*)

Transketolase A combined with Transaldolase reaction (v_{tkata})

$$\frac{V_{f,\mathrm{tkata}}\mathrm{C5P}^{n_{\mathrm{tkata},1}}}{(K_{m,\mathrm{C5P,tkata}}+\mathrm{C5P}^{n_{\mathrm{tkata},1}})\left(K_{\mathrm{AMP,tkata}}+\frac{\mathrm{AMP}}{K_{i,\mathrm{tkata}}}\right)^{n_{\mathrm{tkata},2}}}$$

DAHP synthase (v_{dahps})

$$\frac{\mathbf{V_{max,dahps}PEP\cdot NADPH\cdot E4P}}{\mathbf{A+B}}$$

$$\mathbf{A=K_{m,PEP,dahps}(K_{i,E4P,dahps}K_{i,NADPH,dahps}+K_{i,NADPH,dahps}E4P+K_{i,E4P,dahps}PEP+PEP\ E4P)}$$

$$\mathbf{B=NADPH(K_{i,E4P,dahps}K_{m,PEP,dahps}+K_{m,NADPH,dahps}E4P+K_{m,E4P,dahps}E4P+PEP+NADPH)}$$

Bold terms are omitted after the model reduction.

Table 8
Spline functions for the metabolites, that remain unbalanced (Gluc, ADP, ATP, NAD, NADP and AcCoA)

Gluc		ADP		ATP		NAD		NADP		AcCoA	
Nodes	B-spline coefficients	Nodes	B-spline coefficients	Nodes	B-spline coefficients	Nodes	B-spline coefficients	Nodes	B-spline coefficients	Nodes	B-spline coefficients
−5.0000	0.0631	−5.0000	0.6753	−5.0000	0.4025	−5.0000	2.9660	−5.0000	0.2192	−5.0000	3.6229
−5.0000	0.0421	−5.0000	0.6849	−5.0000	0.4023	−5.0000	2.9857	−5.0000	0.2173	−5.0000	3.6204
−5.0000	0.0995	−5.0000	0.6551	−5.0000	0.4028	−5.0000	2.8846	−5.0000	0.2224	−5.0000	3.6277
0.0000	0.0198	0.0000	0.7086	0.0050	0.4022	0.0000	3.3717	0.0000	0.2139	0.0000	3.6167
0.7000	7.5511	1.0000	0.9044	0.2000	0.1580	5.0000	5.1756	0.4000	0.0531	1.0000	−2.1266
0.8000	13.6257	2.0000	1.4485	1.0000	0.4151	10.0000	0.7978	2.0000	0.1776	2.0000	4.6914
1.5000	15.3896	3.0000	1.1464	3.0000	0.6058	12.0000	5.0259	2.7000	0.1551	10.0000	4.5448
2.4000	10.0773	5.0000	0.0873	6.0000	0.2418	16.5000	4.9967	4.5000	0.2052	15.0000	0.4194
11.0000	16.0859	8.0000	1.6813	8.0000	0.4307			10.0000	0.1197	15.5120	0.0622
17.0000	14.4613	15.0000	1.6808	12.0000	0.2796						
		16.5000	1.2166	16.7020	0.3191			15.3150	0.2463		

A.2. Smoothing splines

Smoothing splines were used for data processing by implementing the routine, e02bac of the NAG C library [36]. This method permits the assignment of weights to the data values to take account of differing accuracy and the number and position of interior knots of the cubic B-splines. The parameter values of the interpolating spline functions are obtained after curve fitting to the data points with respect to the minimum of the sum of the squares of the residuals [37].

The spline functions of the co-metabolites, that were not balanced by the models are given in Table 8.

References

[1] J.W. Lengeler, Metabolic networks: a signal oriented approach to cellular models, Biological Chemistry 381 (2000) 911–920.

[2] R.U. Ibarra, J.S. Erwads, B.O. Palsson, *Escherichia coli* K12 undergoes adaptive evolution to achieve in silico predicted optimal growth, Nature 420 (2002) 186–189.

[3] W. Wiechert, 13C metabolic flux analysis, Metabolic Engineering 3 (2001) 195–303.

[4] M. Tomita, K. Hashimoto, K. Takahashi, T.S. Shimizu, Y. Matsuzaki, F. Miyoshi, K. Saito, S. Tanida, K. Yugi, J.C. Venter, C.A. Hutchinson III, E-cell: a software environment for whole cell simulation, Bioinformatics 15 (1999) 72–84.

[5] H.V. Westerhoff, The silicon cell, not dead but live, Metabolic Engineering 3 (2001) 207–210.

[6] M. Rizzi, M. Baltes, U. Theobald, M. Reuss, In vivo analysis of metabolic dynamics in *Saccharomyces cerevisiae*: II Mathematical model, Biotechnological Bioengeering 55 (4) (1997) 592–608.

[7] U. Schäfer, W. Boos, R. Takors, D. Weuster-Botz, Automated sampling device for monitoring intracellular metabolite dynamics, Analytical Biochemistry 270 (1999) 88–96.

[8] D. Weuster-Botz, Sampling tube device for monitoring intracellular metabolite dynamics, Analytical Biochemistry 246 (1997) 225–233.

[9] A. Buchholz, R. Takors, C. Wandrey, Quantification of intracellular metabolites in *Escherichia coli* K12 using liquid chromatographic-electrospray ionization tandem mass spectrometric techniques, Analytical Biochemistry 295 (2001) 129–137.

[10] I. Schomburg, A. Chang, D. Schomburg, BRENDA, enzyme data and metabolic information, Nucleic Acids Research 30 (2002) 47–49.

[11] R.D. Appel, A. Bairoch, D.F. Hochstrasser, A new generation of information retrieval tools for biologists: the example of the ExPASy WWW server, Trends in Biochemical Sciences 19 (1994) 258–260.

[12] W. Wiechert, R. Takors, Validation of metabolic models: concepts, tools and problems, in: H.V. Westerhoff, B.N. Kholodenko (Eds.), Metabolic Engineering in a Post Genomic Era (in press).

[13] D. Degenring, R. Takors, In vivo investigation of metabolic dynamics in *Escherichia coli* K12 by evaluation of rapid sampling experiments, in: J. Kim (Ed.), Proceedings of the 5th German Workshop on Artificial Life, 2002.

[14] A. Buchholz, Quantitative Untersuchungen intrazellulärer Metabolitdynamiken zur Identifizierung mikrobieller Sto-

ffwechselnetzwerke, Ph.D. Thesis, Friedrich-Wilhelms-Universität Bonn, Germany, 2002.
[15] L. Notley-McRobb, A. Death, T. Ferenci, The relationship between external glucose concentration and cAMP levels inside *Escherichia coli*: implications for models of phosphotransferase-mediated regulation of adenylate cyclase, Microbiology 143 (1997) 1909–1918.
[16] H.R. Kaback, Tergulation of sugar transport in isolated bacterial membrane preparations from *Escherichia coli*, Proceedings of the National Academical Science, USA 63 (1969) 724–731.
[17] P.P. Schmidt, F. Travers, T. Barman, Transient and equilibrium kinetic studies on yeast 3-phosphoglycerate kinase. Evidence that an intermediate containing 1,3-bisphophoglycerate accumulates in the steady-state, Biochemistry 34 (1995) 824–832.
[18] M. Molnar, M. Vas, Mg^{2+} affects the binding of ADP but not ATP to 3-phosphoglycerate kinase. Correlation between equilibrium dialysis binding and enzyme kinetic data, Biochemical Journal 293 (1993) 595–599.
[19] T.G. Spring, F. Wold, The purification and characterization of *Escherichia coli* enolase, Journal of the Biological Chemistry 52 (1971) 6797–6802.
[20] A. Cornish-Bowden, Fundamentals of Enzyme Kinetics, Portland Press, London, 1995.
[21] I. Segel, Enzyme Kinetics Behavior and Analysis of Rapid Equilibrium and Steady-State Enzyme Systems, John Wiley and Sons, New York, 1975.
[22] J.G. Hayes, Numerical methods for curve and surface fitting, Bulletin of the Institute of Mathematics and its Applications 10 (1974) 144–152.
[23] J. Hurlebaus, A. Buchholz, W. Alt, W. Wiechert, R. Takors, MMT—a pathway modeling tool for data from rapid sampling experiments, In Silico Biology 2 (2002) 0042.
[24] A. Saltelli, K. Chan, E.M. Scott, Sensitivity Analysis, John Wiley and Sons, New York, 2000.
[25] T. Turányi, Sensitivity analysis of complex kinetic systems. Tools and applications, Journal of Mathematical Chemistry 5 (1990) 203–248.
[26] K. Mauch, S. Arnold, M. Reuss, Dynamic sensitivity analysis for metabolic systems, Chemical Engineering Science 52 (15) (1997) 2589–2598.
[27] M.D. Haunschild, B. Freisleben, R. Takors, W. Wiechert, Distributed simulation of metabolic networks with model variants, in: Proceedings of the 16th European Simulation Multiconference, 2002, pp. 436–440.
[28] E.P. Dougherty, J.T. Hwang, H. Rabitz, Journal of Chemical Physics 71 (1979) 1794.
[29] C. Seigneur, G. Stephanopoulos, R.W. Carr, Chemical Engineering Science 37 (1982) 845.
[30] I.T. Jolliffe, Discarding variables in a principal component analysis. I: artificial data, Journal of the Royal Statistical Society 21 (1972) 160–172.
[31] T. Turányi, T. Bérces, S. Vajda, Reaction rate analysis of complex kinetic systems, International Journal of Chemical Kinetics 21 (1989) 83–99.
[32] S. Vajda, P. Valkó, T. Turányi, Principal component analysis of kinetic models, International Journal of Chemical Kinetics 17 (1985) 55–81.
[33] C. Chassagnole, N. Noisommit-Rizzi, J.W. Schmid, K. Mauch, M. Reuss, Dynamic modeling of the central carbon metabolism of *Escherichia coli*, Biotechnology and Bioengineering 79 (2002) 53–73.
[34] J.A. Nelder, R. Mead, The downhill simplex method, Computer Journal 7 (1965) 308.
[35] T. Rowan, Functional stability analysis of numerical algorithms, Ph.D. Thesis, University of Texas at Austin, Austin, TX, USA, 1990.
[36] Available from <http://www.nag.com/numeric/cl/CLdescription.asp>.
[37] M.G. Cox, J.G. Hayes, Curve fitting: a guide and suite of algorithms for the non-specialist user. NPL Report NAC 26, National Physical Laboratory, 1973.